Fusion Engineering and Design 199 (2024) 114136

Contents lists available at ScienceDirect

Fusion Engineering and Design

journal homepage: www.elsevier.com/locate/fusengdes

Experimental determination of the solubility of hydrogen in a quality certified eutectic PbLi alloy

Igor Peñalva [a,*], María Urrestizala [a], Jon Azkurreta [a], Natalia Alegría [a], Marta Malo [b], Belit Garcinuño [b], Julián Patiño [b], David Rapisarda [b]

[a] Energy Engineering Department, Bilbao School of Engineering (EIB/BIE), Plaza Ingeniero Torres Quevedo, 1, University of the Basque Country (UPV/EHU), Bilbao 48013, Spain

[b] CIEMAT, Centro de Investigaciones Energéticas y Medioambientales, Avda. Complutense 40, Madrid 28040, Spain

ARTICLE INFO

Keywords:
Eutectic lead-lithium alloy
Tritium
Solubility
Diffusivity
Fusion reactor materials

ABSTRACT

The efficient operation of the liquid breeding blankets relies on the correct definition of the transport parameters of protium, deuterium and tritium in PbLi liquid metals with an eutectic composition. This is the case of the DCLL blanket or the WCLL, where the solubility and diffusivity values will affect to the induced tritium flux in terms of magnitude and kinetics.

However, there exists a huge band in the literature for the results obtained experimentally for the solubility of the isotopes in the mentioned liquid metal alloy, which is unacceptable from the designing point of view. Moreover, the exact content of lithium and the impurities that the PbLi alloy may contain seems to be another key issue that needs to be faced.

This work shows the preliminary results obtained in a new measurement campaign carried out with samples of PbLi qualified in terms of impurities and lithium content. These samples have been tested in the Absorption-Desorption facility of the UPV/EHU that has been recently repaired and upgraded as part of EUROfusion program in collaboration with CIEMAT.

1. Introduction

The liquid breeding blankets to be designed and manufactured in the near future need a proper definition of the protium, deuterium and tritium transport parameters in the PbLi eutectic alloy. The efficient operation of these breeding blankets relies, to a great extent, on this critical issue. This is the case of the dual-coolant lithium-lead breeding blanket (DCLL) or the Water Cooled Lithium Lead (WCLL). Moreover, these parameters will directly affect other factors, such as the design of the tritium extraction systems or the coolant purification system [1,2].

However, despite its relevance, these values have not been defined with certainty. Their study implies several difficulties that lead to uncertainties that can slow down the development of these breeding blankets, which will be crucial components of future fusion reactors. In the particular case of the measurement of the solubility by means of Sieverts' constant (K_S), a very wide range has been documented in the literature for the experimental results [3]. The quality and the exact composition (specifically the presence of impurities and the Li content) in the tested eutectic PbLi alloys may be responsible of this data dispersion [4].

The Fusion Materials Laboratory (FML) of the UPV/EHU has an Isovolumetric Absorption-Desorption facility. This rig has been used for measurements related to hydrogen transport parameters of different materials [5–12]. After an accidental breakdown, it has been recently repaired and upgraded as part of EURO*fusion* program in collaboration with CIEMAT. New samples of the liquid metal (PbLi), qualified in terms of impurities and Li content, have been used during this new campaign.

2. Material

CIEMAT has acquired new batches of the eutectic PbLi alloy to CAMEX GmbH. CIEMAT has also been responsible for analyzing the alloy chemically and has certified its quality in terms of lithium content, together with a quantification of the very low presence of contaminants.

In order to check if the PbLi sample is in eutectic composition, a series of analytical tests have been made in CIEMAT. Firstly, Differential

* Corresponding author.
E-mail address: igor.penalva@ehu.eus (I. Peñalva).

https://doi.org/10.1016/j.fusengdes.2023.114136
Received 13 October 2023; Received in revised form 14 December 2023; Accepted 27 December 2023
Available online 10 January 2024

Table 1
Elemental composition of 4 PbLi samples of the material as analyzed by XRF, together with the lithium content identified by FAES.

Sample	Elemental composition XRF (wt.%)						FAES (wt.%)
	Pb	Al	Ca	Cu	Ni	Others	Li
1	99.270	0.004	–	0.013	0.022	0.019	0.600
2	99.230	–	0.031	0.016	0.030	0.019	0.650
3	99.240	0.010	0.022	0.019	0.021	0.019	0.625
4	99.260	0.009	–	0.013	0.023	0.019	0.577

Thermal Analysis (DTA) and Thermogravimetric (TG) analysis have been carried out. The measurements were made in nitrogen atmosphere from room temperature to 700 °C, showing a peak at about 235 °C that represents the endothermic transition for the melting point of the eutectic PbLi. Then, a chemical analysis determined that the lithium percentage of 14.7 at.% ± 1.99 %, which fits into the range reported for the eutectic composition [13]. X-Ray Diffraction (XRD) technique was also used and the presence of oxides onto the surface was identified. Finally, X-Ray Fluorescence (XRF) was also used to identify and quantify the presence of contaminants and impurities. Table 1 shows the elemental composition for 4 PbLi samples of the material as analyzed by XRF. The lithium content identified by Flame Atomic Emission Spectroscopy (FAES) technique has been added for comparison (XRF technique is not suitable for light elements).

After these analyses were carried out in CIEMAT, the tested sample was sent to the FML in a package under vacuum conditions. The sample was polished using a 120 grit sandpaper inside a glove box under argon atmosphere immediately before mounting into the system, so that any possible surface oxidation or contamination produced during sample handling was eliminated. Additionally, before getting the sample into the Absorption-Desorption facility, and still under an argon atmosphere, the sample was introduced inside the cylindrical tungsten crucible, which was filled with ethanol to avoid the contact of the PbLi with air. This way, the sample was introduced into the Absorption-Desorption facility. Due to the high volatility of the ethanol, it was evaporated during the pumping and heating processes prior to the absorption tests. The sample introduced in the facility weighted 81.36 g. After finishing the tests, a negligible loss of weight of the sample was identified (0.02 g).

3. Experimental

The experimental procedures have already been described before [3, 5]. Here they are briefly summarized for the sake of a correct understanding of the measurements.

A schematic layout of the facility located in the FML is depicted in Fig. 1. In this case, it is very important to minimize the outgassing from the walls. This is why the components selected to build up the rig have been carefully chosen (quartz, commercial glass, etc.). A more detailed description of the facility can be found in Peñalva et al. [3].

The PbLi sample is introduced into the experimental chamber at room temperature (20 °C) inside a cylindrical crucible made of pure tungsten. At this temperature, the liquid metal remains in solid state. The crucible, in turn, rests on a sample holder. This element is made of quartz (see Fig. 2 left). After the mounting process, the PbLi sample stays on the top part of the nose, which is also made of quartz, approximately in the middle of the furnace (see Fig. 2 right). As long as the eutectic PbLi

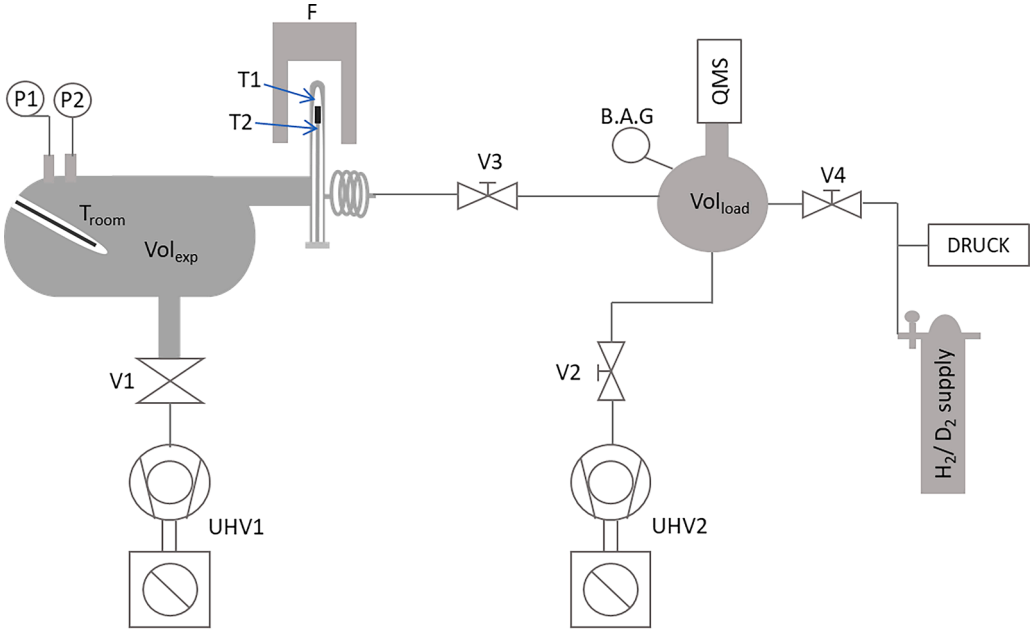

UHV1 and **UHV2**: Ultrahigh Vacuum Pumping Units
V1: Electropneumatic gate valve
V2, V3 and **V4**: Manually actuated gate valves
F: Furnace
P1 and **P2**: Capacitive manometers
T1, T2 and **T3**: Thermocouples

Vol_{exp}: Experimental chamber
Vol_{load}: Loading chamber
QMS: Quadrupole Mass Spectrometer
DRUCK: Absolute pressure transducer
B.A.G.: Bayard-Alpert Gauge

Fig. 1. Schematic layout of the facility [3].

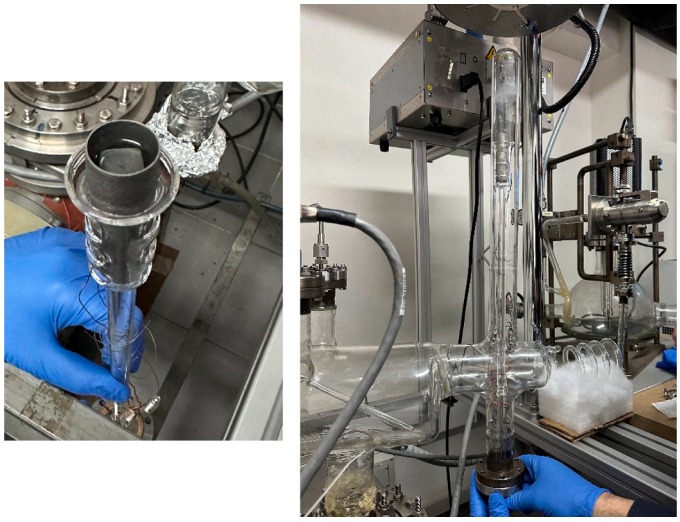

Fig. 2. Photographs of the facility during the mounting process: the PbLi sample is located inside the tungsten crucible, which, in turn, rests on a sample holder made of quartz (left) that is introduced inside the nose made of quartz of the experimental chamber (right) (the cylindrical furnace is not down yet).

alloy melts at ~235 °C, the absorption-desorption processes that will be analyzed later, will take place only through the free surface of the liquid metal sample.

Once ultrahigh vacuum (UHV) conditions have been achieved inside the experimental chamber, an absorption test is carried out at a certain temperature that will remain constant during the whole experiment. This consists of loading the experimental chamber almost instantaneously with the corresponding gas, reaching a certain pressure in the beginning of the absorption experiment. Then, the pressure evolution during a certain loading time (τ_L) is measured. The register of the pressure evolution during this absorption period that normally involves several hours is the basis of the technique: the sample (81.36 g of PbLi in this case) absorbs the loaded gas. The pressure decrease inside the experimental chamber is provoked by the absorption process. This decrease is highlighted by a red line in Fig. 3. The capacitive manometer used for the measurement of the absorption tests is a MKS Type 690A Absolute High Accuracy Pressure Transducer, with a full scale range of 1 Torr, being the resolution 1×10^{-6} of the full scale. It shows an accuracy of 0.12 % of the reading +/- zero/span coefficient. It is important to note that temperatures (room temperature and sample temperature) are controlled continuously and both remain constant during the whole experiment. Besides, before the beginning of each experiment, the experimental chamber is at UHV and the zero of the capacitive manometer is adjusted before loading it. The pressure evolution registered by this device during the loading period can be fitted mathematically to the corresponding theoretical expression, so that the values of the Sieverts' constant and the diffusivity will be obtained from that mathematical regression.

A subsequent desorption run can also be carried out after the described absorption process if the gas of the experimental chamber is quickly removed during a pumping period that takes some seconds (τ_P). This way, the same transport parameters can be obtained by characterizing the desorption phenomenon. However, during this experimental campaign, only absorption measurements have been carried out and blank signals (same experimental conditions but without sample inside the crucible) were subtracted to the experimental values obtained with the sample for each case.

4. Theory

A detailed description of the theoretical model developed expressly

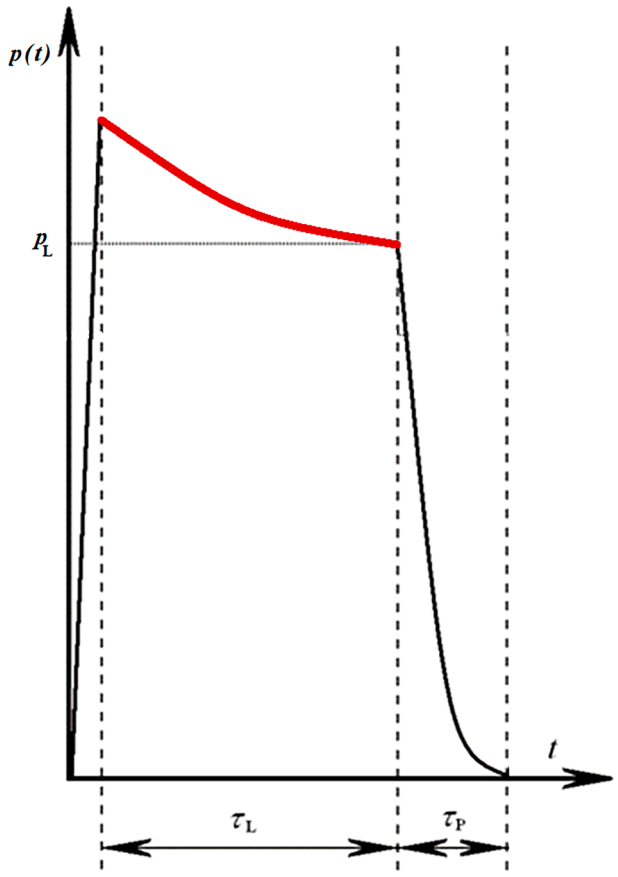

Fig. 3. Experimental phases during an absorption test where the time scale is intentionally distorted in order to make it understandable: the loading time (τ_L) takes several hours whereas the gas entry at the beginning ($t = 0$) and removal (τ_P) are almost instantaneous.

for this equipment has already been described. Thanks to this model, solubility of hydrogen in liquid metals can be experimentally measured, both for absorption and desorption processes. A complete development of the model can be found in Peñalva et al. [3]. Here the model is briefly summarized for the sake of completeness.

Sieverts' law describes the amount of gas dissolved into one sample. For a certain material, it states the proportionality of the gas solubility S (mol m^{-3}) and the partial pressure of the gas p (Pa), according to the Sieverts' constant K_S (mol m^{-3} Pa$^{-0.5}$):

$$S = K_S\, p^{1/2} \tag{1}$$

In thermodynamics, it is common to define Sieverts' constant according to vant Hoffs equation as follows [14–16]:

$$K_S = e^{\left(\frac{-\Delta G_S^0}{R\,T}\right)} = e^{\left(\frac{-\left(\Delta H_S^0 - T\Delta S_S^0\right)}{R\,T}\right)} = e^{\left(\frac{-\left(\Delta H_S^0\right)}{R\,T}\right)}\, e^{\left(\frac{\Delta S_S^0)}{R}\right)} \tag{2}$$

where $\Delta G_S{}^0$ is the standard Gibbs free energy change for solution (J mol^{-1}), R refers to the constant for ideal gases (J K^{-1} mol^{-1}), T is the temperature (K), $\Delta H_S{}^0$ is the standard enthalpy change for solution (J mol^{-1}) and $\Delta S_S{}^0$ is the standard entropy change for solution (J K^{-1} mol^{-1}).

It is important to note that, according to Eq. (2), Sieverts' constant is temperature-dependent and fulfills an Arrhenius equation, which is widely used in fusion materials science as follows [12,17,18]:

$$K_S = K_{S0}\, e^{\left(\frac{-E_S}{R\,T}\right)} \tag{3}$$

Table 2
Conditions and results for the 4 new experimental absorption tests.

Temperature [°C]	Loading Pressure [Pa]	Loading Time [s]	Sieverts' Constant [mol m^{-3} Pa$^{-0.5}$]	RMSE of the Fitting [Pa]
241	24.98	87,326	1.83×10^{-2}	0.108
369	26.14	87,326	1.29×10^{-2}	0.094
475	26.11	87,326	3.18×10^{-2}	0.132
579	26.38	18,616	1.49×10^{-2}	0.048

where K_{S0} is the pre-exponential factor (mol m^{-3} Pa$^{-0.5}$) and E_S states for the activation energy of the solubility (J mol^{-1}). A positive value of the E_S will characterize the material as endothermic. On the contrary, an exothermic material will show a negative value of E_S.

On the other hand, according to Fick's second law in one dimension (x):

$$\frac{\partial c}{\partial t} = D\ \frac{\partial^2 c}{\partial x^2} \tag{4}$$

where c is the concentration of the gas inside the material (mol m^{-3}), variable with time t (s) and position (x), and D refers to the effective diffusivity (m^2 s^{-1}).

The solution to Eq. (4) during the absorption phase for the described geometry and conditions can be written as follows [19]:

$$c_1(x,t) = c_0 - \frac{4\ c_0}{\pi}\ \sum_{n=0}^{\infty}\left[\frac{(-1)^n}{(2\ n+1)}\right] e^{-D\ (2\ n\ +\ 1)^2\ \pi^2 \frac{t}{4\ a^2}} \cos\left[\frac{(2\ n+1)\ \pi\ x}{(2\ a)}\right] \tag{5}$$

where c_o is the initial concentration and a is the height of the free surface of the PbLi from the bottom of the crucible.

On the other hand, Fick's first law allows the calculation of the gas flux J (mol m^{-2} s) in a one-dimensional problem:

$$J(x,t) = -D\frac{\partial c}{\partial x} \tag{6}$$

Eqs. (5) and (6) can be combined for the described geometry and condition and the section A (m^2) of the free surface can be taken into account in order to integrate the flux. This way, the evaluation of the total amount of gas absorbed by the sample can be carried out. Then, taking into account Eq. (1) and considering the volume of the sample (V_S), the moles of gas that have been loaded into the liquid metal sample are calculated. Finally, the ideal gas law allows the conversion of moles into pressure [3]. This way, this is the final expression for this absorption phase:

$$p_N(t) = p_{N,\ L} - \frac{R\ T_N}{V} K_S\ p_L^{\frac{1}{2}}\ V_S\left[1 - \frac{8}{\pi^2}\sum_{n=0}^{\infty}\left[\frac{1}{(2\ n+1)^2}\right] e^{-D\ (2\ n\ +\ 1)^2\ \pi^2\ t/\left(4\ a^2\right)}\right] \tag{7}$$

where $p_{N,L}$ (Pa) is the initial normalized loading pressure, T_N (K) is the normalized temperature, V (m^3) is the volume of the experimental chamber and p_L (Pa) is the loading pressure.

The experimental measurement of the pressure evolution during this absorption process should fit this theoretical equation, which allows the calculation of the transport parameters (K_S and D). As mentioned before, a detailed description of this theoretical model, both for absorption and desorption, can be found in Peñalva et al. [3].

5. Results and discussion

Taking into account the process explained above, a total set of four experimental absorption tests have been carried out, at four different temperatures (241 °C, 369 °C, 475 °C and 579 °C). The first three tests lasted approximately 24 h, whereas for the fourth one, the pressure evolution during the absorption process was registered during approximately 5 h. In all cases hydrogen (protium) was used and the loading

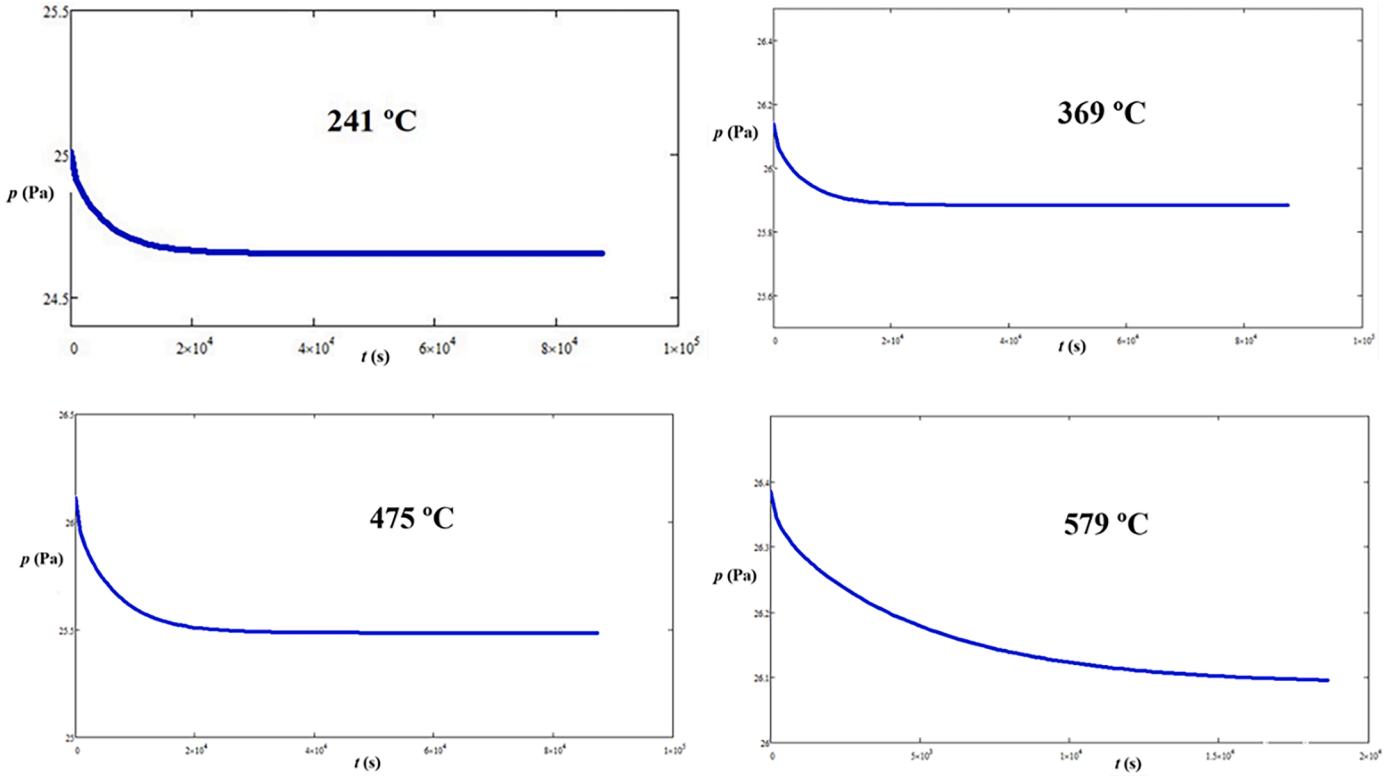

Fig. 4. Fittings to the experimental measurements of the pressure evolution (in Pa) with time (in s) according to Eq. (7) for the 4 new absorption tests.

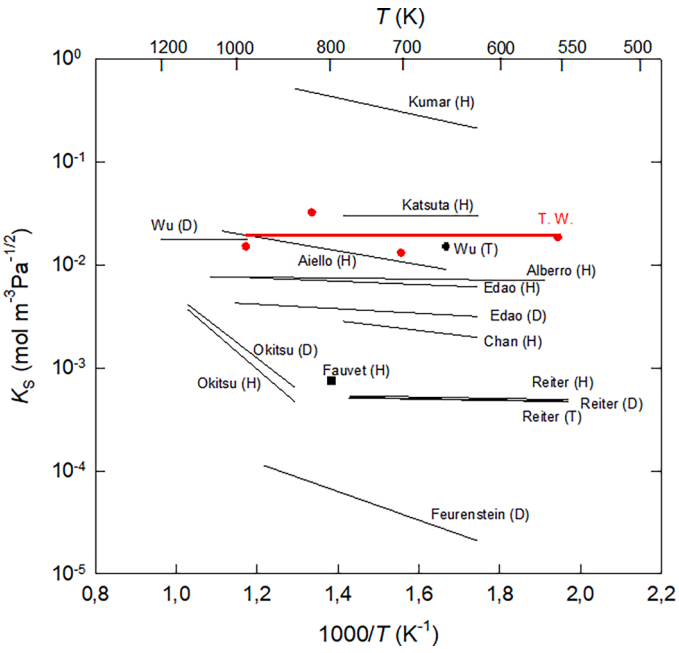

Fig. 5. Experimental measurements of Sieverts' constant in this work (T.W.) compared to literature data [3].

pressure range has been approximately 25–27 Pa (see exact measurements in Table 2). The mathematical fittings to the experimental measurements are shown in Fig. 4. In addition, in order quantify the goodness of the fit, the Root Mean Square Error (RMSE) of each fitting has been calculated (see Table 2).

Results are depicted in Fig. 5, together with some of the references and show almost no variation for the Sieverts' constant with the temperature with an average value of 1,95 × 10^{-2} mol m^{-3} $Pa^{-0.5}$ in the tested temperature range.

These results fit in the middle-up zone of the aforementioned extensive range and are quite close to previous results obtained at the same facility by Alberro et al. [5] or with the ones measured by Edao et al. [20]. These authors reported a slightly smaller solubility and a very little value for the activation energy of the solution process. The solubilities obtained in this campaign are similar to those obtained by Wu [21], Wu et al. [22] and Katsuta et al. [23], with values for the Sieverts' constant that do not depend on temperature. They are also in the range reported by Aiello et al. [17] who reported a high value for the activation energy of the solution process and, as a result, an endothermic Arrhenius dependence of the solubility with the temperature.

These results differ from the ones obtained by Feuerstein et al. [24], Okitsu et al. [25] or Reiter [18], that show lower values for the solubility (one or two orders of magnitude) and with a general endothermic tendency. They also differ from the ones presented by Kumar et al. [26] that report higher values (more than one order of magnitude) and also an endothermic tendency (see Fig. 5).

6. Conclusions

The efficient operation of the liquid breeding blankets relies on the correct definition of the transport parameters of protium, deuterium and tritium in the eutectic PbLi. In this context, given the wide variability of results found in the literature, it is essential to fine-tune the results. For this reason, a new test campaign has been carried out, using new samples of PbLi qualified in terms of impurities and lithium content.

To date, 4 protium absorption tests have been carried out at 4 different temperatures (241 °C, 369 °C, 475 °C and 579 °C) in order to measure the Sieverts' constant in PbLi. Results show almost no variation for the Sieverts' constant with the temperature, with an average value of 1,95 × 10^{-2} mol m^{-3} $Pa^{-0.5}$.

New experimental absorption and desorption campaigns are foreseen in order to confirm the results obtained, on the one hand, and, to analyse the isotopic influence by using protium and deuterium alternatively, on the other. Additionally, an analysis of the PbLi samples is foreseen after the absorption-desorption tests in order to check that the sample has not been contaminated during the measurements and that the eutectic composition remains the same.

CRediT authorship contribution statement

Igor Peñalva: Conceptualization, Data curation, Formal analysis, Funding acquisition, Investigation, Methodology, Supervision, Writing – original draft, Resources. **María Urrestizala:** Conceptualization, Data curation, Formal analysis, Investigation, Methodology, Writing – review & editing. **Jon Azkurreta:** Conceptualization, Data curation, Formal analysis, Investigation, Methodology, Writing – review & editing. **Natalia Alegría:** Funding acquisition, Investigation, Methodology, Writing – review & editing. **Marta Malo:** Conceptualization, Funding acquisition, Investigation, Methodology, Writing – review & editing, Resources. **Belit Garcinuño:** Formal analysis, Investigation, Methodology, Writing – review & editing, Resources. **Julián Patiño:** Investigation, Methodology, Writing – review & editing, Resources. **David Rapisarda:** Funding acquisition, Resources, Writing – review & editing.

Declaration of competing interest

The authors declare that they have no known competing financial interests or personal relationships that could have appeared to influence the work reported in this paper.

Data availability

Data will be made available on request.

Acknowledgment

This work has been carried out within the framework of the EUROfusion Consortium, funded by the European Union via the Euratom Research and Training Programme (Grant Agreement No 101052200 — EUROfusion). Views and opinions expressed are however those of the author(s) only and do not necessarily reflect those of the European Union or the European Commission. Neither the European Union nor the European Commission can be held responsible for them.

References

[1] L.V. Boccaccini, et al., Status of maturation of critical technologies and systems design: breeding blanket, Fusion Eng. Des. 179 (2022) 113116, https://doi.org/10.1016/j.fusengdes.2022.113116.
[2] I. Fernández-Berceruelo, et al., Remarks on the performance of the EU DCLL breeding blanket adapted to DEMO, Fusion Eng. Des. 155 (2020) (2017) 111559, https://doi.org/10.1016/j.fusengdes. 2020.111559.
[3] I. Peñalva, et al., Hydrogen transport model in eutectic PbLi for data evaluation in an absorption-desorption experimental facility, Fusion Sci. Technol. 00 (2023), https://doi.org/10.1080/15361055.2023.2194237.
[4] B. Garcinuño, et al., Establishing technical specifications for PbLi eutectic alloy analysis ant its relevance in fusion applications, Nucl. Mater. Energy 30 (2022) 101146, https://doi.org/10.1016/j.nme.2015.07.021.
[5] G. Alberro, et al., Experimental determination of solubility values for hydrogen isotopes in eutectic Pb-Li, Fusion Eng. Des. 98–99 (2015) 1919–1923, https://doi.org/10.1016/j.fusengdes.2015.05.060.
[6] G.A. Esteban, et al., Study of the isotope effects in the hydrogen transport in polycrystalline tungsten, Mater. Sci. Forums 480-481 (2005) 537–542, https://doi.org/10.4028/www.scientific.net/MSF.480-481.537.
[7] G.A. Esteban, et al., Isotope effect in hydrogen transport in BCC-structured materials: polycrystalline tungsten and reduced activation ferritic-martencitic steel, Fusion Sci. Technol. 48 (2005) 617–620, https://doi.org/10.13182/FST05-A1001.

[8] G.A. Esteban, et al., Characterisation of deuterium transport in the fibers and matrix of a 3D-SiCf/SiC composite, Fusion Eng. Des. 69 (2003) 463–467, https://doi.org/10.1016/D0920-379(03)00103-0.
[9] G.A. Esteban, et al., Deuterium transport in SiCf/SiC composites, J. Nucl. Mater. (2002) 1430–1435, https://doi.org/10.1016/S0022-3115(02)01282-5, 307-311.
[10] G.A. Esteban, et al., Tritium transport characterisation in martensitic steels from isotopic effect studies, Fusion Sci. Technol. 41 (2002) 948–953, https://doi.org/10.13182/FST02-A22725.
[11] G.A. Esteban, et al., Study of isotope effects in the hydrogen transport of an 8% CrWVTa martensitic steel, Phys. Status Solidi 184 (2) (2001) 409–418, https://doi.org/10.1002/1521-396X(200104)184:2<409::AID−PSSA409>3.0.CO;2-K.
[12] G.A. Esteban, et al., Hydrogen isotope diffusive transport parameters in pure polycrystalline tungsten, J. Nucl. Mater. 295 (2001) 49–56, https://doi.org/10.1016/S0022-3115(01)00486-X.
[13] E. Mas De Les Valls, et al., Lead-lithium eutectic material database for nuclear fusion technology, J. Nucl. Mater. 376 (2008) 353–357, https://doi.org/10.1016/j.jnucmat.2008.02.016.
[14] N.D. Deveau, et al., Beyond Sieverts' Law: a comprehensive microkinetic model of hydrogen permeation in dense metal membranes, J. Memb. Sci. 437 (2013) 298–311, https://doi.org/10.1016/j.memsci.2013.02.047.
[15] Y. Su, et al., Hydrogen solubility in molten TiAl alloys, Int. J. Hydrog. Energy 35 (2010) 8008–8013, https://doi.org/10.1016/j.ijhydene.2010.05.054.
[16] N.D. Deveau, et al., Evaluation of hydrogen sorption and permeation parameters in liquid metal membranes via Sieverts' apparatus, Int. J. Hydrog. Energy 43 (2018) 19075–19090, https://doi.org/10.1016/j.ijhydene.2018.08.101.
[17] A. Aiello, et al., Determination of hydrogen solubility in lead lithium using SOLE device, Fusion Eng. Des. 81 (2006) 639–644, https://doi.org/10.1016/j.fusengdes.2005.06.364.
[18] F. Reiter, Solubility and diffusivity of hydrogen isotopes in liquid Pb-17Li, Fusion Eng. Des. 14 (1991) 207–211, https://doi.org/10.1016/0920-3796(91)90003-9.
[19] H.S. Carslaw, J.C. Jaeger, Conduction of Heat in Solids, Clarendon Press, Oxford, 1975.
[20] Y. Edao, et al., Experiments of hydrogen isotope permeation, diffusion and dissolution in Li-Pb, J. Nucl. Mater. 417 (2011) 723–726, https://doi.org/10.1016/j.jnucmat.2010.12.126.
[21] C.H. Wu, The solubility of deuterium in lithium-lead alloys, J. Nucl. Mater. 114 (1983) 30–33, https://doi.org/10.1016/0022-3115(83)90069-7.
[22] C.H. Wu, A.J. Blair, A study of the interaction of tritium with liquis Li17Pb83, in: Proceedings of the 12th Symposium of Fusion Technology, Jülich, Germany September, 1982, pp. 13–17.
[23] H. Katsuta, et al., Hydrogen solubility in liquid Li17Pb83, J. Nucl. Mater. 167 (1985) 167–170, https://doi.org/10.1016/0022-3115(85)90127-8.
[24] H. Feuerstein, et al., Behavior of deuterium and rare gases in thermal convection loops with molten Pb-17Li, Fusion Eng. Des. 14 (1991) 261–271, https://doi.org/10.1016/0920-3796(91)90010-N.
[25] H. Okitsu, et al., Analysis of diffusion and dissolution of two-component hydrogen (H+D) in lead lithium, Fusion Eng. Des. 87 (2012) 1324–1328, https://doi.org/10.1016/j.fusengdes.2012.03.004.
[26] S. Kumar, et al., Studies on the solubility of hydrogen in molten Pb82Li17 eutectic alloy, Int. J. Hydrog. Energy 38 (2013) 6002, https://doi.org/10.1016/j.ijhydene.2013.03.033. -2007.